Vol. 29 (1998) *ACTA PHYSICA POLONICA B* No 1–2

SPIN–ISOSPIN GIANT RESONANCES BY CHARGE EXCHANGE REACTIONS *

M. Fujiwara, I. Daito, H. Fujimura, H. Akimune, T. Inomata, F. Ihara, K. Ishibashi

Research Center for Nuclear Physics, Osaka University
Mihogaoka 10–1 Ibaraki, Osaka, 567, Japan

A. Tamii and M. Yosoi

Department of Physics, Kyoto University
Sakyo, Kyoto 606-01, Japan

(Received November 24, 1997)

Spin–isospin excitations in nuclei studied via the charge exchange reactions are discussed together with some historical remarks concerning with the findings of the spin–isospin giant resonances. Measurements of the singles (^{3}He,t) spectra at zero degrees and studies of proton decays from the spin–isospin excitations are reported. We report results on the complementary (t,^{3}He) measurements. Special topics treated are the Gamow–Teller excitations, the spin flip dipole resonances, and the feature of the alpha cluster structures in light nuclei, which are observed both in the proton decay and in the (t,^{3}He) measurements.

PACS numbers: 24.30. Cz, 25.40. Kv, 27.20. +n, 29.30. Ep

1. Introduction

The nuclear giant resonances are characterized as the broad state exhausting almost all the sum rule values [1, 2]. A typical example of spin–isospin resonances mediated by the operator $\vec{\sigma}\cdot\vec{\tau}$ is the Gamow–Teller giant resonance in ^{208}Bi. An experimental observation of this giant resonance [3,4] is shown in Fig. 1. Spin–isospin excitations in ^{208}Bi are strongly excited using the ^{208}Pb(^{3}He,t)^{208}Bi charge exchange reaction at, and near 0° at $E(^3\text{He})$=450 MeV. Fig. 1 clearly shows the presence of the Gamow–Teller resonance (GTR), the isobaric analog states (IAS) and the spin–flip dipole

* Presented at the XXV Mazurian Lakes School of Physics, Piaski, Poland, August 27–September 6, 1997.

($\Delta L = 1$) resonance (SDR) in ^{208}Bi. The shapes of these resonances exhausting the major part of the sum rule values are well fitted by the Breit–Wigner type function expressed as

$$\sigma(E) \propto \frac{1}{(E - E_{\rm res})^2 + (\Gamma/2)^2}. \tag{1}$$

Here, $E_{\rm res}$ in the Breit–Wigner shape function is the centroid energy of the resonance, and Γ is the resonance width, which is related to the life time τ as $\tau \approx \hbar/\Gamma$.

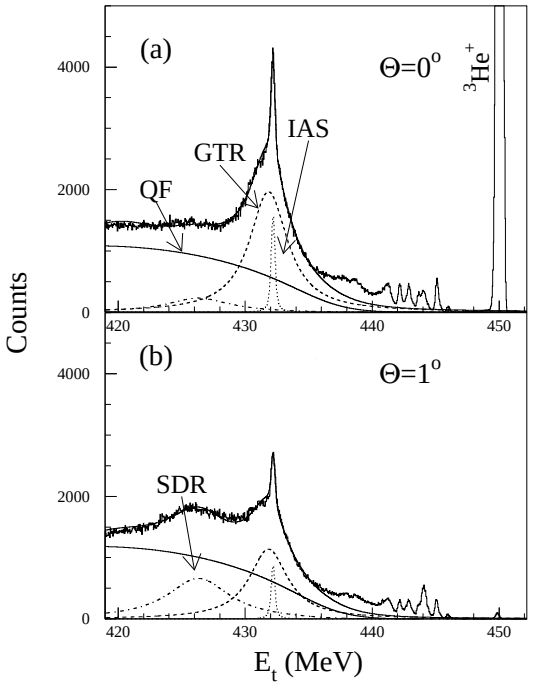


Fig. 1. Experimental triton energy spectra from the ^{208}Pb(^{3}He,t) reaction at E(^{3}He)=450 MeV. (a) Spectrum gated for scattering angles centered at $\theta = 0°$. The IAS, and GTR are prominent. The sharp peak denoted by ^{3}He$^+$ corresponds to the events due to the atomic electron exchange process of ^{3}He$^{++} \rightarrow ^3$He$^+$. The dashed, dotted, dot-dashed and solid lines represent the results of χ^2 fits obtained for the GTR, IAS, SDR and non-resonant background, respectively. (b) Same as (a) but for spectrum gated for scattering angles centered at $\theta = 1°$.

The resonance width Γ is the sum of two different terms consisting of the spreading widths $\Gamma^{\downarrow}$ and the escape width $\Gamma^{\uparrow}$;

$$\Gamma = \Gamma^{\downarrow} + \Gamma^{\uparrow}. \tag{2}$$

Here, the escape width relates to the microscopic, one-proton-particle–one-neutron-hole structure of the resonance. In heavy nuclei, the spreading width is predominantly due to statistical neutron decay because statistical proton decay is strongly suppressed by the Coulomb barrier.

The Gamow–Teller giant resonance (GTGR) is the oscillation to exchange neutrons to protons and to reverse the spin directions as well. This mode of resonances was identified by the (p,n) reactions in 1980's [5–7]. The history concerning the findings of the Gamow–Teller giant resonance is interesting. The Gamow–Teller resonance was first introduced in 1963 to explain the common retardation of the Gamow–Teller (GT) transitions in the allowed β-decay compared with single particle estimates [9, 10]. Subsequently, the analyses of the first forbidden β-decay were made by Ejiri and Fujita [11] in connection with the nuclear core polarization effect. The spin-dipole resonances (SDR) were predicted at the excitation energy higher than those for the GTGR in order to explain the common retardation of the first forbidden β-decay [11]. Empirical finding was retarded; the existence of the GTGR was first reported in 1975 in the $^{90}\mathrm{Zr}(p,n)$ reaction at the incident proton energy of 35 MeV [5].

Historically, the presence of the broad bump corresponding to the GTGR had already been seen by Bowen *et al.,* [12] in 1962 in the 0° (p,n) spectra measured for the several nuclear targets at E_p=143 MeV. Unfortunately almost all the nuclear scientists did not understand the true nature of the bumps seen in the (p,n) spectra for a long time. The broad bumps corresponding to the GTGR were again observed in 1978 in the (p,n) spectra at E_p=800 MeV [13]. This time, the bumps were not correctly interpreted and were identified as the quasielastic charge exchange peaks.

In 1980, the GTGR bumps were correctly interpreted to be preferentially excited at 0° in the (p,n) reactions at the bombarding energy higher than 100 MeV [6–8]. More important is that the (p,n) reaction cross sections leading to the isobaric analog (IAS) and Gamow–Teller states are possible to be related to the β-decay matrix elements using the similarities between the zero-degree charge-exchange reactions and the neutrino capture weak process;

$$\left(\frac{d\sigma}{d\Omega}\right)_{F,\mathrm{GT}}(q{\approx}0,\theta=0^\circ) = \left(\frac{\mu}{\pi\hbar^2}\right)^2\left(\frac{k_f}{k_i}\right)\left[N_\tau\left(J_\tau\right)^2 B(F) + N_{\sigma\tau}\left(J_{\sigma\tau}\right)^2 B(\mathrm{GT})\right], \tag{3}$$

$$\sigma = \left(\pi c^3\hbar^4\right)^{-1}\left[G_V^2\,B(F) + G_A^2\,B(GT)\right]P_e W_e F(eZ, W_e). \tag{4}$$

Since the same operators mediate β-decay and neutrino-capture processes, the cross section of a charge exchange reaction provides a good measure of these weak interaction strengths, if the simple eikonal approximation is valid irrespective of the reaction mechanism. This similarity between the haronic and electro-weak processes allows one to address some important problems in astrophysics. For example, electron capture plays an important role in the evolution of the core of a presupernova star and in the nature of the core collapse that triggers a supernova explosion.

In many electro-weak processes in astrophysics, the transition strength of Gamow–Teller absorption cross sections must be calibrated by analogous processes with charge-exchange reactions. These calibrated transition matrix elements are used in the network chain calculations for the solar evolution processes. Thus, the nuclear giant resonances are sometimes discussed in relation to the astrophysics and the neutrino physics.

In the GT transitions, there are two transition modes; one is the β^- GT transitions mediated by the $\sigma\tau^-$ operator, and another is the β^+ GT transitions mediated by the $\sigma\tau^+$ operator. The sum rule for the β^- and β^+ GT transitions is

$$S_{\beta^-} - S_{\beta^+} = 3(N - Z). \tag{5}$$

This sum rule, sometimes called Ikeda sum-rule, is model-independent. The $\sigma\tau^-$ and $\sigma\tau^+$ operators may act on the spins of quarks in nucleons. Even if the quark spin degree of freedom is taken into account, the Ikeda sum rule is still conserved [2].

2. Charge-exchange reactions

As mentioned above, the presence of the Gamow–Teller giant resonance (GTGR) was first claimed in $^{90}\mathrm{Zr}(p,n)^{90}\mathrm{Nb}$ experiments at 35 MeV at the Michigan State University cyclotron [5]. But, the observed excitation strength was not very evident to give a clear credit for the presence of the giant resonance. This situation completely changed after the installation of a neutron time-of-flight facility at Indiana University Cyclotron Facility (IUCF). Above the bombarding energy higher than E_p=100 MeV, the Gamow–Teller resonances were strongly excited and systematically observed in almost all nuclei [6, 7, 14]. The strong excitations of the GT states at intermediate energies are due to the advantage that the isovector central components of the effective interactions $\mathrm{V}_{\sigma\tau}$ associated with charge-exchange reactions are relatively strong at $E_p \geq 100$ MeV and that the contribution of the tensor and spin-orbit components is generally small at forward angles [15, 16].

The GTGR was also studied via alternative charge-exchange reactions like (^{3}He,t) and (^{6}Li,^{6}He) taking advantage of high resolution and 100% de-

tection efficiency. In particular, the (^{3}He,t) reaction has been used to observe the GT strengths at various bombarding energies $E \leq 100$ MeV/u [17–24]. However, it is now understood that the analysis of the (^{3}He,t) reaction at $E \leq 100$ MeV is more difficult than for the (p, n) reaction at $E \geq 100$ MeV due to strong contributions from the non-central interaction, although the behavior of the (^{3}He,t) reaction as a function of the bombarding energy is not clear yet. The (^{3}He,t) reaction becomes an important alternative to investigate spin–isospin excitations for bombarding energies $E \geq 100$ MeV.

This situation has been demonstrated by the (^{3}He,t) work at Saclay [25], and recently at RCNP [26]. Especially, the newly installed spectrometer "Grand Raiden" (see Fig. 2) becomes a good tool to study the spin–isospin excitations in nuclei [27]. The large magnetic rigidity of the spectrometer allows to measure the (^{3}He,t) spectra at 150 MeV/A in coincidence with particle-decays.

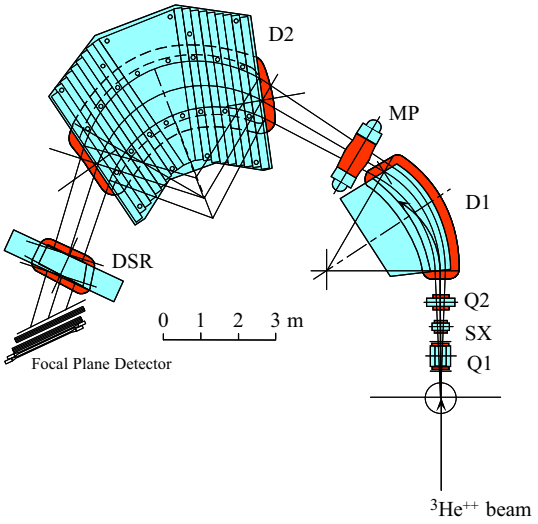


Fig. 2. Schematic layout of the spectrometer Grand Raiden. The paths of the central ray and two extreme rays are shown. The notations D1 and D2 are the first and second dipole magnets. Q1, Q2: first and second quadrupole magnets. SX: sextupole magnet. DSR: dipole magnet for spin rotation measurements. MP: multipole field magnet. The ^{3}He^{++} beam is stopped at the Faraday cup at the inside of the D1 magnet. Tritons are detected by the focal plane detector. For details, see Ref. [27].

A comparison between ^{58}Ni(^{3}He,t) and ^{58}Ni(p, n) spectra measured at 450 MeV and 160 MeV, respectively, shows a close correspondence [28]. Therefore, (^{3}He,t) spectra measured at 0° and 450 MeV provide a probe to determine GT strengths in nuclei as an alternative and powerful probe

compared to (p, n) reactions. This is because triton particles can be detected in magnetic analyzer with 100% detection efficiency and with high energy resolution. With the advantage of high resolution, the (^{3}He,t) cross sections at 0° are used to extract the isospin information from the comparison with the M1 strength distribution obtained by (e, e') measurements. Such a comparison [29] is shown in Fig. 3. Analogous transition strengths are observed in the two spectra, especially in the region of E_x∼8 MeV, where the $T = 1$, 1^+ states are expected.

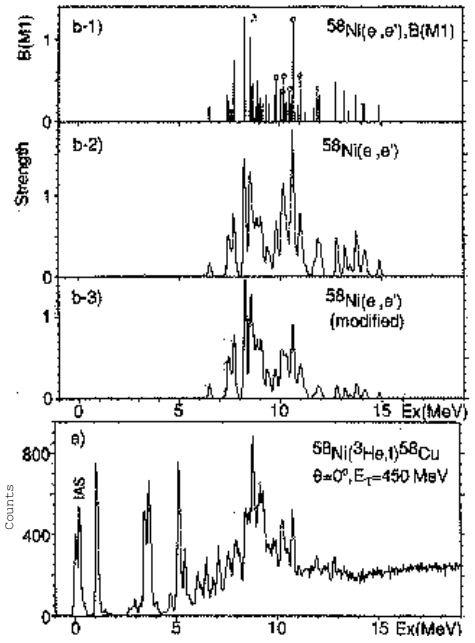


Fig. 3. Comparison between the 0° ^{58}Ni(^{3}He,t) spectrum and the M1 strength distribution obtained in the (e, e') experiment. (a) The 0° ^{58}Ni(^{3}He,t) spectrum. (b-1) The B(M1)↑ strength distribution in ^{58}Ni. (b–2) The reconstructed B(M1) spectrum convoluted with the experimental energy resolution of the (^{3}He,t) measurement. (b–3) The same as (b–2), but the M1 strengths with $T = T_0$+1 are reduced by a factor of three. For details, see Ref. [29].

The ground state of ^{58}Ni has the isospin T_0=1. In charge-exchange reactions, the excitation strength ratio of $\frac{2T_0-1}{2T_0+1}$:$\frac{1}{T_0+1}$: $\frac{1}{(2T_0+1)(T_0+1)}$=2:3:1 is expected for the GT states with the T_0-1, T_0, and T_0+1, respectively, from the isospin coupling consideration. In the M1 excitations via the ^{58}Ni(e, e') reaction, the corresponding ratio is 1:1. Thus, in order to compare the M1 and GT strengths, the strengths in B(M1) must be corrected. In fact, if we artificially reduce the strengths of the M1 states with $T_0 + 1$ by a factor

of three, the global shape becomes similar to each other. The similarity in excitation strength of M1 and GT states indicates that the Gamow–Teller and M1 transitions are predominantly excited by the same $\sigma\tau$ operator.

In general, the M1 states in the (e, e') reaction are dominantly excited by the spin and orbital parts: $\frac{1}{2}(g_s^p - g_s^n)\vec{\sigma}\cdot\vec{\tau} + (g_l^p - g_l^n)\vec{l}\cdot\vec{\tau}$, while the Gamow–Teller operator is $(g_s^p - g_s^n)\vec{\sigma}\cdot\vec{\tau}$. In addition, the contributions from isobar and meson exchange currents are expected in the M1 excitation. Thus, the detailed comparisons of the M1 and GT states excited via (e, e'), (p, p') and charge-exchange reactions would be very useful to study the non-negligible role of the orbital part, meson exchange parts and the Δ-hole contribution [30, 32], although we need a stringent test of the wave function of the states through the shell-model calculations.

3. Gamow–Teller transitions to the β^+ side

The (n, p) type charge exchange reactions with high resolution are particularly important for astrophysics. For example, in electron capture processes in the supernova explosion, the low-lying discrete Gamow–Teller (GT_+) states play an important role. The GT_+ states are pushed down to the low-lying excitations due to the attractive force of the particle-particle residual interactions, and the GT_+ strengths are relatively strong near the ground states.

The (t,^{3}He) charge-exchange reaction has good advantages to be used as an important extension of the (n, p) charge-exchange reaction [33–35], primarily because of expected improved beam qualities compared with those of neutron beams. If high-resolution measurements of charge-exchange reactions of the (n, p) type (ΔT_z=+1) become possible at intermediate energies, significant contributions are expected to the study of astrophysical processes [36] as well as double β-decay processes. However, there exists no accelerator with a dedicated tritium ion source for projectiles of $\geq$100 MeV/u.

Recently, such (t,^{3}He) experiments were performed with the radioactive-beam facility at the National Superconducting Cyclotron Laboratory (NSCL) [37]. The primary 620 MeV ^{4}He beam from the K1200 cyclotron bombarded the metallic beryllium production target with a thickness of 9.25 g/cm^2 mounted in the target position located at the entrance of the A1200 system. The A1200 system was used in a dispersion-matched mode [38], and the triton particles were transported in a dispersive mode to the targets for (t,^{3}He) reactions at this intermediate image position. The energy spread of tritons passing through the first half of the A1200 system to the reaction target was estimated to be $\sim$23 MeV. This energy broadening was cancelled out and the final (t,^{3}He) spectra were obtained with a good resolution.

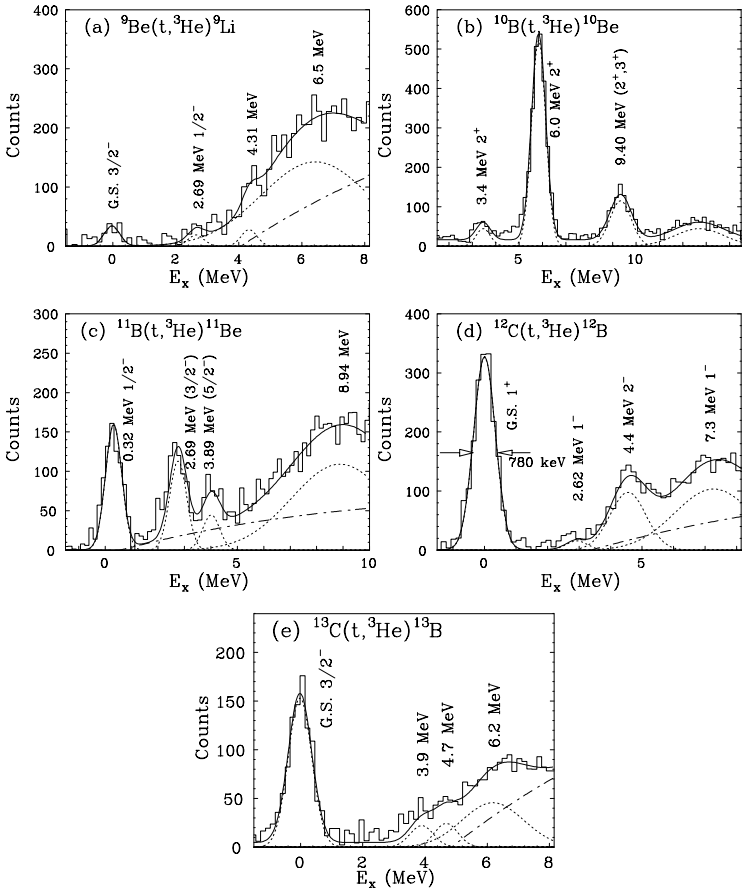


Fig. 4. (t,^{3}He) spectra at zero degrees taken with a triton beam of 381 MeV. The dispersion matching method in charged-particle optics is applied to correct the energy width of ∼23 MeV for the initial triton beam from the breakup (^{4}He,p-t) reaction. The solid and dotted curves are the results of peak fitting. The dot-dashed curves are the non-resonant quasi-free background.

Spectra in Fig. 4 show the results of the 0° (t,^{3}He) measurements on ^{9}Be, ^{10}B, ^{11}B, ^{12}C, and ^{13}C. The GT states in ^{10}Be are interesting. In the ^{10}B(t,^{3}He)^{10}Be spectrum (shown in Fig. 4(b)), we recognized three strong peaks and one broad peak at E_x=3.37 MeV, 5.96 MeV, 9.4 MeV, and 12 MeV. The peaks at 3.37 MeV and 5.96 MeV correspond to the GT transitions from the 3$^+$ ground states of ^{10}B to the 2^+_1 and 2^+_2 states in ^{10}Be. It is very natural to assume that the spin-parity of the 9.4 MeV state is most likely 3^+_1, since the shell model calculation predicts the presence of a strong GT transition to a 3^+_1 state at ∼9 MeV in the mirror nucleus ^{10}C [39]. A definite spin-parity

assignment, however, cannot be made for the 9 MeV state from the present experiment, and the possibility of a 2^+ assignment cannot be excluded. The nature of the broad peak at E_x≈12 MeV is not clear at present.

The 0° cross sections for a pure GT transition can be factorized as [7,25],

$$\left(\frac{d\sigma}{d\Omega}\right)(\theta = 0^\circ) = \left(\frac{\mu}{\pi\hbar^2}\right)^2 \frac{k_f}{k_i} \left[N_{\sigma\tau} \mid J_{\sigma\tau} \mid^2 B(\mathrm{GT})\right], \qquad (6)$$

where μ is the reduced mass, k_i and k_f are the initial and final momenta, $J_{\sigma\tau}$ is the volume integral of the $\sigma\tau$ component of the effective nucleon-nucleus interaction, $B(GT)$ is the GT strength, and $N_{\sigma\tau}$ is a distortion factor which is the ratio of the cross sections calculated in the distorted- and plane-wave Born approximations. The above proportionality is confirmed by taking into account the distortion factor as $N_{\sigma\tau}$=exp(-0.81$A^{1/3}$). The distortion effect in the (t,^{3}He) reaction at 127 MeV/A seems to be slightly larger than is the case for the (^{3}He,t) reaction at 450 MeV [26]. The value of the volume integral for the effective spin–isospin interaction was $J_{\sigma\tau}$ ≈160 MeV·fm^3 for (^{3}He,t), and it was found to be $J_{\sigma\tau}$ ≈153±10 MeV·fm^3 for (t,^{3}He). These values are consistent with theoretical predictions. By using the effective interaction and the distortion factors deduced for the present experiment

TABLE I

Comparison of the zero-degree (t,^{3}He) cross sections and B(GT) values. The B(GT) values are deduced from experimental β decay log*ft* values (normalization) and from the measured 0° (t,^{3}He) cross sections.

Target (J^π)	Residual(J^π, E_x) (MeV)	B(GT)	$d\sigma/d\Omega$ (mb/sr)
^{9}Be($3/2^-$)	^{9}Li($3/2^-$, g.s.)	0.019[a]	0.27±0.07
^{10}B(3^+)	^{10}Be(2_1^+, 3.37)	0.08±0.03[b]	1.0± 0.3
^{10}B(3^+)	^{10}Be(2_2^+, 5.96)	0.95±0.13[b]	12.0± 0.8
^{10}B(3^+)	^{10}Be((2^+ or 3^+), 9.4)	0.31±0.08[b]	3.9± 0.7
^{11}B($3/2^-$)	^{11}Be($1/2^-$, 0.3)	0.23±0.05[b]	2.8± 0.4
^{11}B($3/2^-$)	^{11}Be(($3/2^-$), 2.7)	0.17±0.05[b]	2.1± 0.4
^{11}B($3/2^-$)	^{11}Be(($5/2^-$), 3.8)	0.07±0.03[b]	0.84±0.3
^{12}C(0^+)	^{12}B(1^+, g.s)	0.999±0.005[a]	11.8± 1.4
^{13}C($1/2^-$)	^{13}B($3/2^-$, g.s)	0.759±0.018[a]	9.6± 0.9

[a] Deduced from the β decay log*ft* values (Ref. [40]).

[b] Experimental results from the present (t,^{3}He) measurements.

from the transitions with known B(GT) values to the ground states of ^{9}Li ($3/2^{-}$), ^{12}B (1^{+}), and ^{13}B ($3/2^{-}$), we estimated the B(GT) values for the other GT states. They are listed in Table I together with the known B(GT) values from the β decay studies.

The GT and M1 transitions in the A=10 system are especially interesting in view of isobaric mirrors. The three states at 3.37 MeV, 5.96 MeV and 9.4 MeV are excited (see Fig. 4(b)) in the ^{10}B(t,^{3}He)^{10}Be reaction at θ=0°. These three states in ^{10}Be are inferred to be spin–isospin flip GT ($\Delta S = 1$, $\Delta T = 1$) states. In the DWBA analyses of the 2_1^+ and 2_2^+ states (E_x = 3.35 and 5.3 MeV) in ^{10}C observed in the mirror ^{10}B$(p,n)^{10}$C reaction at E_p=186 MeV, Wang *et al.* [39] show that the corresponding transitions to these two states are dominated by ΔJ^{π}=1^{+} transition.

In Fig. 5, a new isobar diagram for $T = 1$ mirror GT and M1 states is proposed for the $A = 10$ system by taking into account the compilation of energy level data [40]. The 2_1^+ states at 3.37 MeV in ^{10}Be, at 5.17 MeV in ^{10}B, and at 3.35 MeV in ^{10}C are mirror states. The 2_2^+ states at 5.9 MeV in ^{10}Be, at 7.48 MeV in ^{10}B, and at 5.3 MeV in ^{10}C also constitute mirror states. These 2_2^+ states are excited with strong GT and M1 strengths. The M1 strength from the 3^+ to 2_2^+ states in ^{10}B is measured as B(M1)= 1.745 μ_N^2 [31]. From this value, we can estimate the expected B(GT) values for the corresponding mirror states in ^{10}Be and ^{10}C by neglecting possible contributions from orbital excitations and from the isobar and meson exchange currents [32]. The value of B(GT)=B(M1)/2.64μ_N^2=0.66 agrees with the measured value B(GT$_-$)=0.68±0.02 obtained in the ^{10}B$(p,n)^{10}$C experiment [39]. On the other hand, the value measured in the present experiment of B(GT$_+$)=0.95±0.13 to the 2_2^+ mirror state at 5.9 MeV is larger.

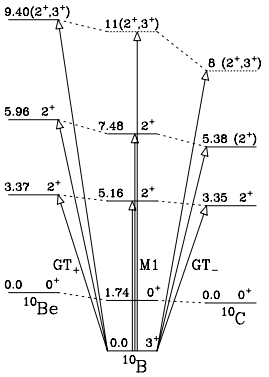


Fig. 5. Isobar diagram for states with the GT$_+$, M1, and GT$_-$ transitions from the ^{10}B ground state. The strong transitions in ^{10}Be, ^{10}B, and ^{10}C are indicated by the arrows. The mirror candidates of the 9.4 MeV state in ^{10}B are indicated at 11 MeV in ^{10}B, and at 8 MeV state in ^{10}C.

This isospin symmetry violation would be possible if the nuclear structure differs between ^{10}C and ^{10}Be due to the presence of the Coulomb force. It would be interesting to determine whether or not the recent elaborate theories expressed in Ref. [41, 42] can predict the observed difference.

The recent theoretical calculation in the framework of the anti-symmetrized molecular dynamics (AMD) predicts that the ^{10}C nucleus consists of two alpha clusters and two valence protons (see Fig. 6) [42]. The mirror ^{10}Be nucleus consists of two alpha clusters and two valence neutrons. As schematically shown in Fig. 6, the Coulomb repulsive force acts to separate the two protons in ^{10}C, if the valence protons locate in a special (0,1,0) orbit as predicted in Ref. [42]. These special situation originated from the alpha cluster structures in the A=10 isobar nuclei may result in a large difference between the GT_+ and GT_- transition strengths from the ^{10}B ground state.

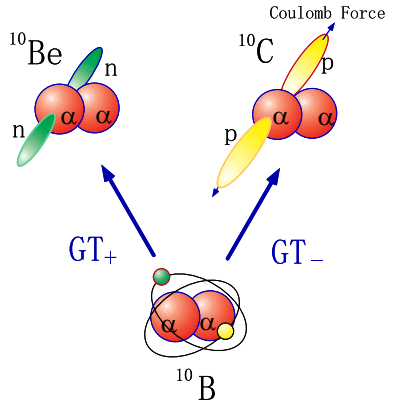


Fig. 6. Schematic explanation of the Gamow–Teller transitions from ^{10}B. A simple alpha cluster model predicts that ^{10}C consists of two α particles surrounded by two valence protons in a (0,1,0) orbit in terms of harmonic-oscillator orbits (n_x, n_y, n_z). For details, see Ref. [42]. ^{10}Be is the isobaric mirror nucleus, in which two neutrons are in the (0,1,0) orbit without any effects from the Coulomb force.

Another question which is not understood is the presence of the strong 3_1^+ (or 2^+) state at ∼9 MeV in ^{10}Be, which is also predicted in a shell-model calculation [39]. Since there is no experimental evidence for corresponding 3^+ (or 2^+) states in both in ^{10}B and ^{10}C, further high resolution studies of inelastic proton scattering and charge-exchange reactions on ^{10}B would be necessary to establish the isobar relation of M1 and GT excitations in the $A = 10$ system.

4. Decay from the spin–isospin resonance in ^{13}N

In view of the α cluster physics, the ground state of ^{13}C is considered to have a structure consisting of three alpha's and one neutron. On the base of this extremely simple picture for the ^{13}C ground state, the charge exchange reaction leads to the ^{13}N states consisting of three alpha's and one protons. If the states in ^{13}N with an α cluster structure different from the ground state of ^{12}C are excited, a valence proton decays to the α cluster states in ^{12}C. A typical example is the 0^+ state at 7.6 MeV in ^{12}C, which is believed to have a acute- or obtuse-angle triangle combination consisting of three α clusters.

On the other hand, the simple shell-model picture predicts that the final states in ^{13}N have a configuration with nucleons in the $p_{1/2}$, $p_{3/2}$ and *sd* orbits. Protons decay from the levels in ^{13}N populates to the final states in ^{12}C with the $(1\nu p_{1/2}, 1\nu p_{3/2}^{-1})$ configuration. This simple configuration cannot make any J^π=0^+ states in ^{12}C. Observation of a level which has a relatively weak proton decay to the ground state of ^{12}C could be a good indication that the level has a $(1\nu p_{1/2}, 1\nu p_{3/2}^{-1})$ configuration. This situation is schematically explained in Fig. 7. Thus, it is very interesting to observe proton decays from the excited levels in ^{13}N excited by the (^{3}He,t) reaction since information obtained from the proton decay data [43] gives a severe limit to check the validity of the nuclear models.

Fig. 8 shows a two dimensional scatter plot of decay protons obtained in coincidence with tritons gated on the (^{3}He,t) reaction at 450 MeV at θ=0°. A singles spectrum measured at the same time is compared with the scatter-plot of decay protons (see Fig. 8(b)). Several sharp states in ^{13}N are strongly excited. The overall shape of the singles (^{3}He,t) spectrum at θ=0° is quite similar to that of the ^{13}C$(p,n)^{13}$N reaction at 200 MeV [45]. There are several clear loci of proton decays from the discrete levels in ^{13}N. It is worth noting that proton decay to the low-lying states in ^{12}C does occur even from highly excited continuum states. This indicates that there are some resonances above E_x=15 MeV. In fact, there is clear indication of the presence of the broad peaks in the excitation energy region at E_x = 17∼24 MeV, which are not mentioned in the (p,n) work by Mildenberger *et al.* [45].

On the base of the schematic model, the possible resonances should have the structure with one neutron in the $p_{1/2}$ orbital coupled to the spin dipole resonances with J^π=0^-, 1^- and 2^-. Thus, the expected resonances above the 15.6 MeV $3/2^-$, $T = 3/2$ state are the $2^-\otimes p_{1/2}$, $1^-\otimes p_{1/2}$, and $0^-\otimes p_{1/2}$ states. This leads to five states as the spin–flip dipole resonance in ^{13}N. These resonances correspond to the SDR in ^{12}N coupled with one neutron, which apparently should be strongly excited by charge-exchange reactions.

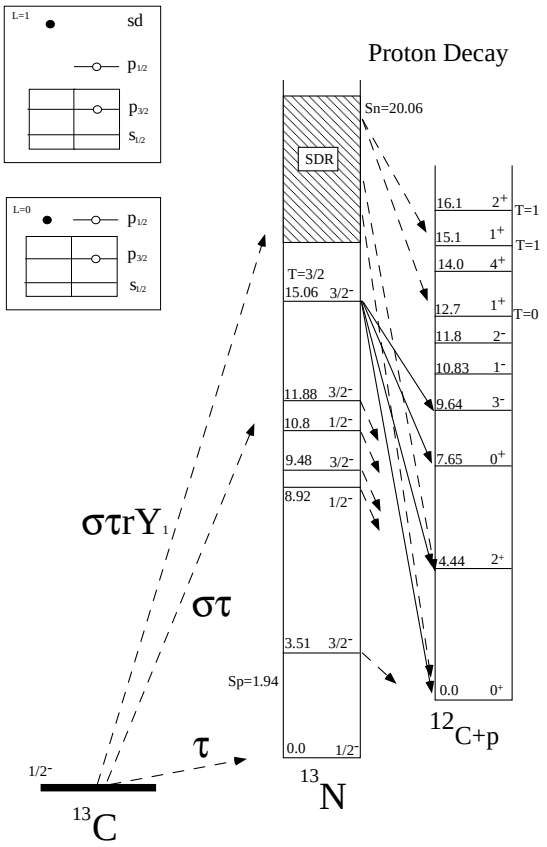


Fig. 7. Level scheme for proton decays from the excited states in ^{13}N. Schematic particle-hole configurations of the excited states are shown at the upper left side. Protons decay from the p-orbit in the case of the states excited with the transferred angular momentum $L = 0$. Protons in the sd-orbits emitted in the case of the SDR resonances excited with $L = 1$.

The observed two-dimensional plot in Fig. 8(a) clearly shows that there are proton decays from the resonances above E_x=15 MeV to some specific states in ^{12}C. Among them, the decay strength to the ground state of ^{12}C is relatively weak compared with that to the 4.4 MeV 2^+ state. Proton decays from the high-lying resonances certainly occur to the 1^+ states at 12.71 and 15.1 MeV, which predominantly have the one-particle one-hole $(1\nu p_{1/2}, 1\nu p^{-1}_{3/2})$ configuration. This indicates that the resonances above 15 MeV have a configuration consisting of one proton particle in the *sd* orbits and one neutron and one neutron-hole in the $p_{1/2}$ and $p_{3/2}$ orbits, respectively.

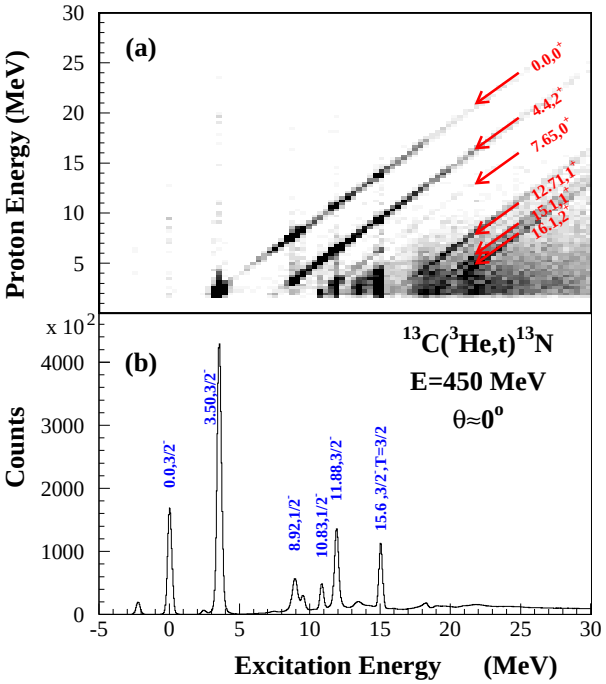


Fig. 8. (a) Two dimensional scatter plot for coincidence events of proton energy versus triton energy (in the unit of excitation energy) gated on scattering angles centered at $\theta = 0°$. Proton decay is measured at $\theta = 160°$. The loci indicate decay of states in ^{13}N by protons to final states in ^{12}C. (b) Singles ^{13}C(^{3}He,t)^{13} spectrum measured at E(^{3}He)=450 MeV, $\theta = 0°$. For details, see [44].

Of interest is that the proton decay from the 10.83 MeV $1/2^-$ state does not occur into the ground state in ^{12}C, and this state has a strong decay width to the second 0^+ state in ^{12}C. Since the second 0^+ state is inferred to have a three α-cluster structure different from the ground 0^+ state of ^{12}C, the 10.83 MeV, $1/2^-$ state is considered to have a similar α-cluster structure. We again need to await further theoretical efforts for a better understanding of these new observations.

5. Summary

The study of the spin–isospin giant resonances in nuclei was triggered by the beta decay analyses. In the early stage, interest was focused on the discoveries of the resonances. The spin–isospin resonances are, however, found to be mostly important in view of astrophysics and neutrino physics. Some interesting questions should be still addressed for the presence of new

resonances. Can we find the double Gamow–Teller resonance? Does the spin–dipole resonance in a deformed nucleus split into two components like in the case of a giant dipole resonance? What is the mass dependence of these resonances mentioned above? What is the microscopic structure of these spin–isospin resonances? There are several questions which need further experimental efforts in future.

One of the common movements of investigations at the present is toward to understand the dumping mechanism of the resonances (the origin of the width) and the microscopic structures (wave functions). The study of "microscopic structure" of the giant resonances is addressed as the next generation of nuclear physics developments, where the efficient coincidence measurements are indispensable. In the present report, we mainly show the recent results on the spin–isospin excitations in light nuclei. The experimental results strongly indicate that the GT transitions and proton decays are an excellent tool to study the α-cluster and microscopic structures of light nuclei.

The present work was supported in part by a Grant in Aid of Scientific Research, Ministry of Education, Science, Sports and Culture (Monbusho) with grant number 07404012. We like to thank many collaborators in the (^{3}He,t) and (t,^{3}He) work. We especially thank Prof. Ejiri to encourage our work.

REFERENCES

[1] *Electric and Magnetic Giant Resonances in Nuclei,* ed. J. Speth, World Scientific, 1991.

[2] F. Osterfeld, *Rev. Mod. Phys.* **64**, 491 (1992).

[3] H. Akimune, I. Daito, Y. Fujita, M. Fujiwara, M.B. Greenfield, M.N. Harakeh, T. Inomata, J. Jänecke, K. Katori, S. Nakayama, H. Sakai, Y. Sakemi, M. Tanaka, M. Yosoi, *Phys. Lett.* **B323**, 107 (1994).

[4] H. Akimune, I. Daito, Y. Fujita, M. Fujiwara, M.B. Greenfield, M.N. Harakeh, T. Inomata, J. Jänecke, K. Katori, S. Nakayama, H. Sakai, Y. Sakemi, M. Tanaka, M. Yosoi, *Phys. Rev.* **C52**, 604 (1995).

[5] R.R. Doering, A. Galonsky, D.M. Patterson, G.F. Bertsch, *Phys. Rev. Lett.* **35**, 1691 (1975).

[6] D.E. Bainum, J. Rapaport, C.D. Goodman, D.J. Horen, C.C. Foster, M.B. Greenfield, C.A. Goulding, *Phys. Rev. Lett.* **44**, 1751 (1980).

[7] C.D. Goodman, C.A. Goulding, M.B. Greenfield, J. Rapaport, D.E. Bainum, C.C. Foster, W.G. Love, F.P. Petrovich, *Phys. Rev. Lett.* **44**, 1755 (1980).

[8] D.J. Horen *et al.*, *Phys. Lett.* **B95**, 27 (1980).

[9] K. Ikeda, S. Fujii, J.I. Fujita, *Phys. Lett.* **3**, 271 (1963).

[10] J.I. Fujita, K. Ikeda, *Nucl. Phys.* **67**, 145 (1965).

[11] H. Ejiri, K. Ikeda, J.I. Fujita, *Phys. Rev.* **176**, 1277 (1968); H. Ejiri, J.I. Fujita, *Phys. Rep.* **38C**, 85 (1978).

[12] P.H. Bowen, C. Cox, G. Huxtable, J.P. Scanlon, J.J. Thresher, A. Langsford, *Nucl. Phys.* **30**, 475 (1962).

[13] B.E. Bonner, J.E. Simmons, C.R. Newsom, P.J. Riley, G. Glass, J.C. Hiebert, Mahavir Jain, L.C. Nortcliffe, *Phys. Rev.* **C18**, 1418 (1978).

[14] C. Gaarde, *J. Phys.* **45**, C4–405 (1984).

[15] F. Petrovich, J.A. Carr, H. MacManus, *Annu. Rev. Nucl. Part. Sci.* **36**, 29 (1986).

[16] W.G. Love, K. Nakayama, M.A. Franey, *Phys. Rev. Lett.* **28**, 1401 (1981).

[17] A. Galonsky, J.P. Didelez, A. Djaloeis, W. Oelert, *Phys. Lett.* **74B**, 176 (1978).

[18] D. Ovazza, A. Willis, M. Morlet, N. Marty, P. Martin, P. de Saintingnon, M. Buenerd, *Phys. Rev.* **C18**, 2438 (1978).

[19] C. Gaarde, J.S. Larsen, M.N. Harakeh, S.Y. van der Werf, M. Igarashi, A. Müller–Arnke, *Nucl. Phys.* **A334**, 248 (1980); C. Gaarde, J.S. Larsen, A.G. Drentje, M.N. Harakeh, S.Y. van der Werf, A. Müller-Arnke, *Nucl. Phys.* **A346**, 497 (1980).

[20] S.L. Tabor, G. Neuschaefer, J.A. Carr, F. Petrovitch, C.C. Chang, A. Guterman, M.T. Collins, D.L. Friesel, C. Glover, S.Y. van der Werf, S. Raman, *Nucl. Phys.* **A422**, 12 (1984).

[21] W.A. Sterrenburg, M.N. Harakeh, S.Y. van der Werf, A. van der Woude, *Nucl. Phys.* **A405**, 109 (1983).

[22] S.Y. van der Werf, S. Brandenburg, P. Gradijk, W.A. Sterrenburg, M.N. Harakeh, M.B. Greenfield, B.A. Brown, M. Fujiwara, *Nucl. Phys.* **A496**, 305 (1989).

[23] J. Jänecke, F.D. Becchetti, A.M. van der Berg, G.P.A. Berg, G. Brouwer, M.B. Greenfield, M.N. Harakeh, M.A. Hofstee, A. Nadasen, D.A. Roberts, R. Sawafta, J.M. Schippers, E.J. Stephenson, D.P. Stewart, S.Y. van der Werf, *Nucl. Phys.* **A526**, 1 (1991); J. Jänecke, K. Pham, D.A. Roberts, D. Stewart, M.N. Harakeh, G.P.A. Berg, C.C. Foster, J.E. Lisantti, R. Sawafta, E.J. Stephenson, A.M. van der Berg, S.Y. van der Werf, S.E. Muraviev, M.H. Urin, *Phys. Rev.* **C48**, 2828 (1993).

[24] K. Pham, J. Jänecke, D.A. Roberts, M.N. Harakeh, G.P.A. Berg, S. Chang, J. Liu, E.J. Stephenson, B.F. Davis, H. Akimune, M. Fujiwara, *Phys. Rev.* **C51**, 526 (1995).

[25] I. Bergqvist, A. Brockstedt, L. Carlén, L.P. Ekström, B. Jakobsson, C. Ellegaard, C. Gaarde, J.S. Larsen, C.D. Goodman, M. Bedjidian, D. Contrado, J.Y. Grossiord, A. Guichard, R. Haroutunian, J.R. Pizzi, D. Bachelier, J.L. Boyard, T. Hennino, J.C. Jourdain, M. Roy-Stephan, M. Boivin, P. Radvanyi, *Nucl. Phys.* **A469**, 669 (1987).

[26] M. Fujiwara, H. Akimune, I. Daito, H. Ejiri, M.B. Greenfield, M.N. Harakeh, T. Inomata, J. Jänecke, S. Nakayama, N. Takemura, A. Tamii, M. Tanaka, H. Toyokawa, M. Yosoi, *Nucl. Phys.* **A599**, 223c (1996).

[27] M. Fujiwara, in Proceedings of the 5th French–Japanese Symposium on Nuclear Physics, eds. by K. Shimizu and O. Hashimoto, Dogashima, Japan, September 26–30, 1989, p.348.

[28] H. Akimune, I. Daito, Y. Fujita, M. Fujiwara, M.B. Greenfield, M.N. Harakeh, T. Inomata, J. Jänecke, K. Katori, S. Nakayama, H. Sakai, Y. Sakemi, M. Tanaka, M. Yosoi, *Nucl. Phys.* **A567**, 245c (1994).

[29] Y. Fujita, H. Akimune, I. Daito, M. Fujiwara, M.N. Harakeh, T. Inomata, J. Jänecke, K. Katori, C. Lüttge, S. Nakayama, P. von Neumann–Cosel, A. Richter, A. Tamii, M. Tanaka, H. Toyokawa, H. Ueno, M. Yosoi, *Phys. Lett.* **B365**, 29 (1996).

[30] Y. Fujita, H. Akimune, I. Daito, M. Fujiwara, M.N. Harakeh, T. Inomata, J. Jänecke, K. Katori, C. Lüttge, S. Nakayama, P. von Neumann–Cosel, A. Richter, A. Tamii, M. Tanaka, H. Toyokawa, H. Ueno, M. Yosoi, *Phys. Rev.* **C55**, 1137 (1997).

[31] E.J. Ansaldo, J.C. Bergstrom, R. Yen, H.S. Caplan, *Nucl. Phys.* **A322**, 237 (1979).

[32] A. Richter, A. Weiss, O. Häusser, B.A. Brown, *Phys. Rev. Lett.* **65**, 2519 (1990).

[33] K.P. Jackson, A. Celler, Proc. of "Spin Observables of Nuclear Probes", ed. C.J. Horowitz, C.D. Goodman and G.E. Walker, Plenum, New York, 1988, p. 139.

[34] T. Rönnqvist, H. Condé, N. Ollson, E. Ramström, R. Zorro, J. Blomgren, A. Håkansson, A. Ringbom, G. Tibell, O. Jonsson, L. Nilsson,P.-U. Renberg, S.Y. van der Werf, W. Unkelbach, F.D. Brady, *Nucl. Phys.* **A563**, 225 (1993).

[35] N. Olsson, H. Condé, E. Ramstöm, T. Rönnqvist, R. Zorro, J. Blomgren, A. Håkansson, G. Tibel, O. Jonsson, L. Nilsson, P.-U. Renberg, A. Brockstedt, P. Ekström, M. Österlund, S.Y. van der Werf, D.J. Millener, G. Szeflinska, Z. Szeflinski, *Nucl. Phys.* **A559**, 368 (1993).

[36] H.A. Bethe, G.E. Brown, J. Applegate, J.M. Lattimer, *Nucl. Phys.* **A324**, 487 (1979).

[37] B.M. Sherrill, *Nucl. Phys.* **A616**, 145 (1997).

[38] I. Daito, H. Akimune, S.M. Austin, D. Bazin, G.P.A. Berg, J.A. Brown, D.S. Davis, Y. Fujita, H. Fujimura, M. Fujiwara, R. Hazama, T. Inomata, K. Ishibashi, J. Jänecke, S. Nakayama, K. Pham, D.A. Roberts, B.M. Sherrill, M. Steiner, A. Tamii, M. Tanaka, H. Toyokawa, M. Yosoi, *Nucl. Instrum. Methods*, in print.

[39] L. Wang, X. Yang, J. Rapaport, C.D. Goodman, C.C. Foster, Y. Wang, R.A. Lindgern, E. Sugarbaker, D. Marchlenski, S. de Lucia, B. Luther, L. Rybarcyk, T.N. Taddeucci, B.K. Park, *Phys. Rev.* **C47**, 2123 (1993).

[40] F. Ajzenberg–Selve, *Nucl. Phys.* bf A490, 1 (1988); **A506**, 1 (1990); **A523**, 1 (1991).

[41] T. Hosino, H. Sagawa, A. Arima, *Nucl. Phys.* **A523**, 228 (1991) and references therein.

[42] Y. Kanada–En'yo, H. Horiuchi, *Phys. Rev.* **C55**, 2860 (1997).

[43] Preliminaly data are shown by M. Fujiwara *et al.*, in: Proceedings of International workshop on Physics with Recoil Separators and Detector Arrays, eds. by R.K. Bhowmik and A.K. Sinha, New Deli, January 30–February 2, 1995, Allied Publishing Ltd.

[44] H. Fujimura *et al.,* RCNP annual report 1996, p. 4.

[45] J.L. Mildenberger, W.P. Alford, A. Celler, O. Häusser, K.P. Jackson, B. Larson, B. Pointon, A. Trudel, M.C. Vetterli, S. Yen, *Phys. Rev.* **C43**, 1777 (1991).